

Towards a Tighter Bound on Possible-Rendezvous Areas: Preliminary Results

Arun Sharma
sharm485@umn.edu
University of Minnesota, Twin Cities
Minneapolis, Minnesota, USA

Jayant Gupta
gupta423@umn.edu
University of Minnesota, Twin Cities
Minneapolis, Minnesota, USA

Subhankar Ghosh
ghosh117@umn.edu
University of Minnesota, Twin Cities
Minneapolis, Minnesota, USA

ABSTRACT

Given trajectories with gaps, we investigate methods to tighten spatial bounds on areas (e.g., nodes in a spatial network) where possible rendezvous activity could have occurred. The problem is important for reducing the onerous amount of manual effort to post-process possible rendezvous areas using satellite imagery and has many societal applications to improve public safety, security, and health. The problem of rendezvous detection is challenging due to the difficulty of interpreting missing data within a trajectory gap and the very high cost of detecting gaps in such a large volume of location data. Most recent literature presents formal models, namely space-time prism, to track an object's rendezvous patterns within trajectory gaps on a spatial network. However, the bounds derived from the space-time prism are rather loose, resulting in unnecessarily extensive post-processing manual effort. To address these limitations, we propose a Time Slicing-based Gap-Aware Rendezvous Detection (TGARD) algorithm to tighten the spatial bounds in spatial networks. We propose a Dual Convergence TGARD (DC-TGARD) algorithm to improve computational efficiency using a bi-directional pruning approach. Theoretical results show the proposed spatial bounds on the area of possible rendezvous are tighter than that from related work (space-time prism). Experimental results on synthetic and real-world spatial networks (e.g., road networks) show that the proposed DC-TGARD is more scalable than the TGARD algorithm.

CCS CONCEPTS

• Information Systems; • Geographic Information Systems; • Computing Methodologies; • Spatial and Physical Reasoning;

KEYWORDS

Spatio-Temporal Data Analysis, Trajectory Data Mining, Spatial Modeling and Reasoning

ACM Reference Format:

Arun Sharma, Jayant Gupta, and Subhankar Ghosh. 2022. Towards a Tighter Bound on Possible-Rendezvous Areas: Preliminary Results. In *Proceedings of*

November 1-4, 2022 (SIGSPATIAL '22 November 1-4, 2022). ACM, New York, NY, USA, 11 pages. <https://doi.org/XXXXXXX.XXXXXXX>

1 INTRODUCTION

Given trajectories with gaps (i.e., missing data), we investigate methods to tighten bounds on the spatial networks (e.g., road network, river network, etc.) for detecting potential rendezvous or meetup locations. Figure 1 (a) shows a pair of trajectory gaps on an underlying spatial network topology where a gap exists from $t = 2$ to $t = 6$ for both trajectory 1 (blue) and trajectory 2 (red) with a given object speed at 1 unit/second. Current approaches output possible meeting locations of two objects via the intersection of two space-time prisms. For instance, Figure 1 (b) shows six interpolated nodes (green) that qualify as rendezvous locations for both objects. Figure 1(c) shows the result after a time slicing method has reduced the number of nodes (by a factor of 3), filtering out nodes N_{10} , N_{17} , N_{12} , and N_{19} (yellow) and leaving N_{11} and N_{18} (green) as the output. The resultant interpolated nodes are then sent to human analysts for further investigation.

Reducing the size of the space with possible rendezvous nodes is important for helping human analysts to detect and analyze trajectory data gaps. The smaller spatial area can be more effectively verified with ground truth via satellite imagery which can further aid early-stage decision-making. The problem has many societal applications related to homeland security, public health and safety etc. For instance, maritime safety involves monitoring activities such as illegal fishing and illegal oil transfers and transshipments [1]. Similarly, public health officials can analyze a given affected area where two objects could have met to control the potential spread of the disease. This paper focuses on the specific use case of improving public safety when two objects intentionally mask their movements to meet secretly within a trajectory gap area.

The problem is challenging since it is hard to model and interpret specific behavioral patterns, especially the rendezvous of two or more objects within a trajectory gap. Many methods rely on linear interpolation, which may lead to many missed patterns since moving objects do not always travel in a straight path. Methods based on the space-time prism are more geometrically accurate but identify large spatial regions, resulting in a time-intensive operation for the post-processing step performed by the human analyst. Further, such methods have a high computation cost due to large data volume. This work proposes computationally efficient time-slicing methods to effectively capture rendezvous regions with tighter spatial bounds in spatial networks.

The traditional literature [3, 28] on the mobility patterns of objects in spatial networks considers realistic scenarios and events

Permission to make digital or hard copies of all or part of this work for personal or classroom use is granted without fee provided that copies are not made or distributed for profit or commercial advantage and that copies bear this notice and the full citation on the first page. Copyrights for components of this work owned by others than ACM must be honored. Abstracting with credit is permitted. To copy otherwise, or republish, to post on servers or to redistribute to lists, requires prior specific permission and/or a fee. Request permissions from permissions@acm.org.

SIGSPATIAL '22 November 1-4, 2022, Seattle, USA,

© 2022 Association for Computing Machinery.
ACM ISBN 978-1-4503-XXXX-X/18/06...\$15.00
<https://doi.org/XXXXXXX.XXXXXXX>

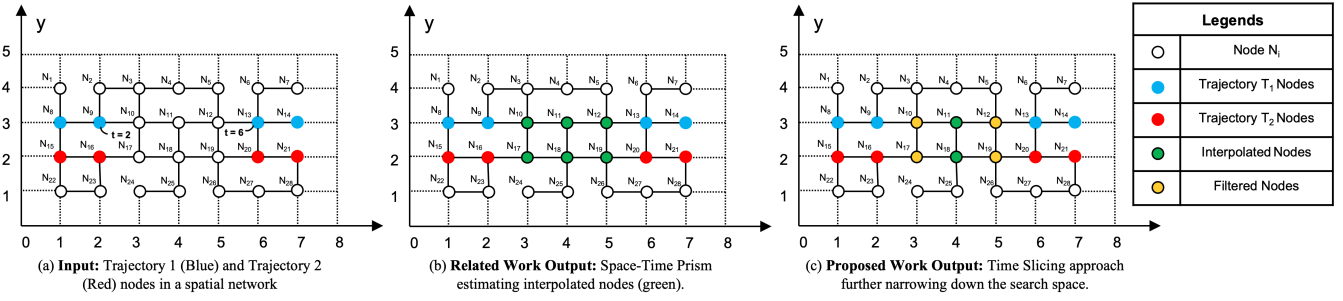


Figure 1: A illustration of Rendezvous Region Detection in Spatial Networks (Best in color)

(e.g., traffic congestion) and other behavioral patterns [6]. However, little attention has been given to movement patterns within trajectory gaps. Most works in this area are limited to linear interpolation methods using shortest path discovery [5, 24]. Other works consider an object’s motion uncertainty via geometric-based methods (e.g., space-time prisms [13, 15, 17]) using spatial geo-ellipse boundaries constructed via motion parameters (e.g., speed). One recent work [23] does explicitly consider rendezvous or meetup queries in a spatial network, which the authors call *assembly queries*, but they used a loosely bounded geo-ellipse estimation from the space-time prism model. Our work proposes time-slicing methods to give tighter bounds on a given rendezvous region and provide further computational speedup using a dual convergence approach.

Contributions: The paper contributions are as follows:

- We propose a time slicing model and theoretically show that it provides a tighter bound on possible rendezvous area relative to traditional space-time prisms.
- Using the time slicing model, we propose a Time Slicing-based Gap-Aware Rendezvous Detection (TGARD) algorithm to effectively detect rendezvous nodes and a Dual Convergence TGARD (DC-TGARD) algorithm using bi-directional pruning to improve the computational efficiency.
- We provide a theoretical evaluation for both algorithms based on correctness, completeness, and time complexity.
- We validate both algorithms experimentally based on solution quality and computation efficiency on both synthetic and real-world datasets.

Scope: The paper proposes TGARD and DC-TGARD algorithms to tighten the spatial bounds of the rendezvous region in the spatial networks. We do not consider gaps with short time intervals (i.e., minutes, seconds etc.) or spatial areas that are low density or sparse. Kinetic prisms [14] fall outside the scope of the paper. In addition, we do not model the rendezvous of the object’s in trajectories without gaps. The proposed framework has multiple phases (i.e., filter, refinement, and calibration), but we limit this work to the filter phase. The refinement phase requires input from a human analyst and is not addressed here, and calibration of the cost model parameters is outside the scope.

Organization: The paper is organized as follows: Section 2 introduces basic concepts, framework and the problem statement. Section 3 provides an overview of time slicing model. Section 4 describes the baseline TGARD and refined DC-TGARD algorithms. Section 5 shows theoretical evaluations for proposed algorithms based on correctness, completeness and asymptotic complexity.

Experimental evaluations are presented for both algorithms and related work are presented in Section 6. A broad and detailed literature survey is given in Section 7. Finally, Section 8 concludes this work and briefly lists the future work.

2 PROBLEM FORMULATION

2.1 Framework

We aim to identify possible rendezvous locations in a given set of trajectory gaps through a two-phase *Filter* and *Refine* approach. We introduce an intermediate time slicing filter to reduce number of interpolated nodes residing within the rendezvous region via proposed algorithms in a computationally efficient manner. The refinement phase further improves the solution quality so that human analysts may extract and analyze a comparatively fewer number of nodes involved in possible rendezvous by two (or more) objects. The inspection is further verified via satellite imagery to derive a possible hypothesis about the rendezvous activity (as shown in Figure 2).

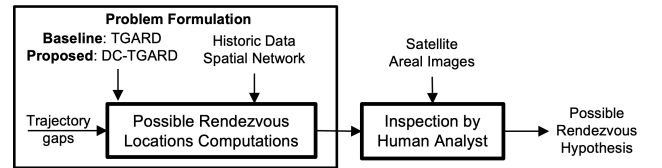


Figure 2: Framework for detecting possible rendezvous locations

2.2 Basic Concepts

A **spatial network** $G = (N, \mathcal{E})$ consists of a node-set N and an edge set \mathcal{E} , where each element $N \in N$ is a geo-referenced point, while each element $E \in \mathcal{E} \subseteq N \times N$ has an edge weight E_w i.e., the minimum time to travel from node N_i to node N_j . Figure 1 shows a spatial network where circles represent nodes (e.g., N_1) and the lines represent edges. A road system is an example of a spatial network where nodes are intersections, and edges are segments.

A **trajectory gap** (G_i) is a spatial interpolated region within a missing location signal time period or Effective Missing Period (EMP) above a certain threshold θ (e.g., 30 mins) between two consecutive points. Such interpolated region can be modeled as a geo-ellipse on the x-y plane, which spatially delimits the extent of a moving object’s mobility given a maximum speed (MS) and effective missing signal period (EMP) (e.g., 30 mins etc) [17]. Figure

3 shows trajectory gap as spatial interpolated region in the form of a geo-ellipse (in blue) with C_1 and C_2 as foci and $t_e - t_s$ (≥ 0) as *EMP* with MS_i as maximum speed.

A **possible rendezvous region** is defined as a set of overlapping nodes and edges when two trajectory gaps (i.e., spatially estimated in the form of geo-ellipse) involving different objects intersect with each other. Hence, such nodes can be defined as **possible rendezvous locations** for a set of objects within a trajectory gap. For instance, Figure 1 (b) shows interpolated nodes (in green) which may involved in a possible rendezvous location derived from the intersection of the two ellipses (as shown in Figure 4) using a space-time prism based method [23] from trajectory T_1 and T_2 .

2.3 Problem Formulation

The problem to optimally identify a trajectory gap region in a spatio-temporal domain is formulated as follows:

Input:

- (1) A Spatial Network
- (2) A set of $|N|$ Trajectory Gaps
- (3) Historic Traffic Data.

Output: A more tightly bound Possible Rendezvous Region

Objective: Solution Quality and Computational Efficiency

Constraints: (1) Trajectories have long gaps (2) Maximum Acceleration is not available (3) Correctness and Completeness

Figure 1 (a) shows the input as a two-dimensional representation of a trajectory gap. Figure 1 (b) shows the output based on intersection of geo-ellipses resulting in interpolated nodes in green. Figure 1 (c) provides a more refined output resulting in a smaller number of interpolated nodes for human analysts to inspect.

3 TIME SLICING MODEL

Our time slicing model uses a space-time prisms [17] to provide a detailed representation of an object's physical space. We first describe space-time prisms and then describe the time slicing model.

Space-Time (ST) Prisms [17] are a collection of spatial points bounded by a physical space which is represented as an interpolated region where moving objects could have passed at a given maximum speed MS . Figure 3 shows the ellipse region in blue for a given time range $[t_s, t_e]$ where t_s denote the start time and t_e denote the end time of the trajectory gap G_i . Equation 1 defines the geo-ellipse with foci (x_s, y_s) and (x_e, y_e) for a missing period $t_e - t_s$ as follows:

$$\sqrt{(x - x_s)^2 + (y - y_s)^2} + \sqrt{(x - x_e)^2 + (y - y_e)^2} \leq (t_e - t_s) \times MS_1 \quad (1)$$

where, (x_s, y_s) and (x_e, y_e) are the start and end points of the trajectory gap with start time t_s and end time t_e ($t_e > t_s$). The ellipse spatially delimits the extent of a moving object's mobility with maximum speed MS_1 .

Figure 4 shows the possible rendezvous region where we perform the spatial intersection of two ellipses $Ellipse_1 \in G_1$ and $Ellipse_2 \in G_2$ and time range is the calculated via inequality 2,

$$[t_s^{Ellipse_1}, t_e^{Ellipse_1}] \cap [t_s^{Ellipse_2}, t_e^{Ellipse_2}] \neq \emptyset \quad (2)$$

A **Time Slice** is an object's physical space sampled within a geo-ellipse (i.e., a ST-Prism) of a trajectory gap. A time slice bounds the spatial intersection of two circles C_1 and C_2 at a given time

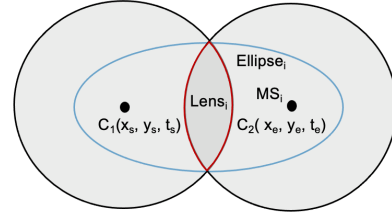


Figure 3: Time Slicing Model with Lens at time instant t

instant t where $t_s \leq t \leq t_e$. Equations 3 and 4 represent the two circles generated from (x_s, y_s) and (x_e, y_e) at given time instant t (where $t_s \leq t \leq t_e$) as follows:

$$C_1 : (x_i - x_s)^2 + (y_i - y_s)^2 \leq (t - t_s)^2 MS_1^2 \quad (3)$$

$$C_2 : (x_i - x_e)^2 + (y_i - y_e)^2 \leq (t_e - t)^2 MS_2^2 \quad (4)$$

Figure 3 shows the spatial bounds of a time slice denoted as *Lens* which is defined as the geometry derived via $C_1 \cap C_2$ at a given time instant t . For instance, $Lens_i$ within an ellipse $Ellipse_i$ generated via maximum speed MS_i at time $t \in [t_s, t_e]$ i.e.,

$$t_s \leq t \leq t_e \quad (5)$$

$$0 \leq MS_1(t - t_s) \leq MS_1(t_e - t_s) \quad (6)$$

$$0 \leq MS_2(t_e - t) \leq MS_2(t_e - t_s) \quad (7)$$

Subtracting Inequality 6 and 7, we get inequality 8 which provides condition to define a lens $Lens_i$ as follows i.e., whether the radii intersection of $C_1 \cap C_2 \geq 0$.

$$MS_1(t - t_s) - MS_2(t_e - t) \geq 0 \quad (8)$$

The bounded region in Figure 3 shows $Lens_i$ i.e., intersection of $C_1 \cap C_2 \geq 0$. The bounded rendezvous regions at a given time instant t is shown in Figure 4 with intersection of $Lens_1$ and $Lens_2 \subseteq Ellipse_1 \cap Ellipse_2$.

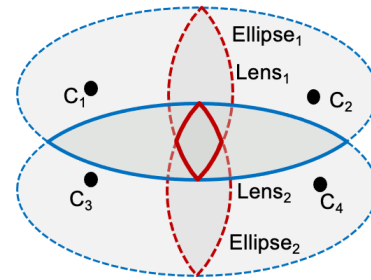


Figure 4: Time slicing model with lens intersection at time instant t

A rendezvous region using a time slicing model is defined as the intersection of $Lens_i$ and $Lens_j$ derived from $Ellipse_1 \in G_1$ and $Ellipse_2 \in G_1$. Figure 4 further represents the rendezvous region via $Lens_1 \cap Lens_2$ at a given time instant t which provides an even tighter bound as compared to the $Ellipse_1 \cap Ellipse_2$. Lemma 3.1 and Lemma 3.2 provide formal proofs to the Theorem 3.3 which states that a time slice is a subset of the intersection of two space time prisms.

LEMMA 3.1. *Given a pair $\langle G_1, G_2 \rangle$ of gaps in trajectories in an isometric euclidean space, the space-time prism model bounds the area of possible rendezvous by the intersection of two ellipses $Ellipse_1$ and $Ellipse_2$ where $Ellipse_1$ specifies the possible locations during gap G_1 given maximum speed MS_1 and $Ellipse_2$ specifies the possible locations during gap G_2 given maximum speed MS_2 .*

Proof. The proof is straightforward. Given a pair of intersecting trajectory gaps G_1 and G_2 , any possible point $P \in \{Ellipse_1, Ellipse_2\}$ such that $Ellipse_1(P) \geq 0$ and $Ellipse_2(P) \geq 0$ must also satisfies inequality 2. Using the inequality 2, P spatially qualifies within possible rendezvous location bounded by Equation 9:

$$Ellipse_1 \cap Ellipse_2(P) \geq 0 \subseteq \{Ellipse_1, Ellipse_2\} \quad (9)$$

Equation 9 shows a possible rendezvous area via intersection of $Ellipse_1$ and $Ellipse_2 \subseteq \{Ellipse_1, Ellipse_2\}$ where $Ellipse_1(P) \geq 0$ and $Ellipse_2(P) \geq 0$. Hence, the intersection of space-time prisms bounds the area of possible rendezvous. \square

LEMMA 3.2. *Given a pair $\langle G_1, G_2 \rangle$ of gaps in trajectories in isometric euclidean space, the time slicing model bounds the instantaneous area of possible rendezvous at time t within the gap time interval by the intersection of $Lens_1$ and $Lens_2$ where $Lens_1$ specifies possible locations during gap G_1 given maximum speed MS_1 and $Lens_2$ specifies possible locations during gap G_2 given maximum speed MS_2 .*

Proof. The circle intersection condition $C_1 \cap C_2 \geq 0$ is already satisfied from Inequality 8. We can extend Inequality 10 and 11 for $Lens_1$ and $Lens_2$ respectively at a given time t :

$$MS_1(t - t_s) - MS_1(t_e - t) \geq 0 \quad (10)$$

$$MS_2(t - t_s) - MS_2(t_e - t) \geq 0 \quad (11)$$

Inequalities 10 and 11 qualifies any point P such that $Lens_1(P) \geq 0$ and $Lens_2(P) \geq 0$. Using Lemma 3.1, any point $P \in Lens_1 \cap Lens_2 \subseteq Ellipse_1 \cap Ellipse_2 \subseteq \{Ellipse_1, Ellipse_2\}$ is bounded by instantaneous time t . \square

THEOREM 3.3. *Given a pair $\langle G_1, G_2 \rangle$ of trajectory gaps in isometric euclidean space, the possible rendezvous area (i.e., lens intersection) bounded at any instant during the gap time interval is a subset of the possible rendezvous area (i.e., ellipse intersection) bounded by the space-time prism model.*

Proof. Given points (x_s, y_s, t_s) and (x_e, y_e, t_e) are focii of the ellipse E . According to Equation 1, a point (x, y) can lie anywhere in the geo-ellipse such that sum of distance from focii (x_s, y_s) and $(x_e, y_e) \leq (t_e - t_s)$. Equation 12 below derived from addition of Equation 3 and 4 of two circles also denotes a property of the ellipse.

$$(x_i - x_s)^2 + (y_i - y_s)^2 + (x_i - x_e)^2 + (y_i - y_e)^2 \leq 2(t_s - t_e)^2 \times MS_i^2 \quad (12)$$

The left hand side of Inequality 12 also denotes each $Lens_i$ is valid $\forall t \in t_s \leq t_i \leq t_e$:

$$\bigcup_{t=t_s}^{t_e} Lens_t \subseteq \bigcup_{t=t_s}^{t_e} (t_s - t_e)^2 \times MS_i^2 \quad (13)$$

In addition, using Lemma 3.1, and 3.2, the areal bounds defined by $Lens_i$ will not exceed the bounds defined by the geo-ellipse. \square

These lemmas and theorems can easily be generalized to spatial networks (e.g., road networks) by generalizing the ellipses and lenses to the subgraphs reachable during a gap time interval and

the subgraphs reachable at a particular time instant within a gap time interval respectively, given a gap-start node, gap-end node, maximum speed and a gap time-interval. Due to lack of space, we are omitting the detailed proofs.

4 PROPOSED APPROACH

In this section, we first explain some underlying concepts which are later used to define the output of the problem (i.e., *possible rendezvous nodes*) in spatial networks. We then discuss the required pre-processing steps related to gathering candidate trajectory gap pairs which are later temporally sampled to construct spatial sub-networks. Finally, we present our proposed TGARD and DC-TGARD algorithms which leverage time slicing properties for better solution quality and computational efficiency.

To calculate possible rendezvous locations, we first estimate the *availability interval* for each object and then calculate how early that object is able to reach (i.e., *earliest arrival time*) and the latest time the object can depart (*latest departure time*) at a given node. We formally define them as follows:

An **Earliest Arrival Time** (N_i^{EA}) is the minimum time object O_i takes from start node N_s to an intermediate node N_u i.e., $N_u^{EA} = N_s^{EA} + E_w$. A **Latest Departure Time** (N_i^{LA}) is the minimum time the object O_i takes from end node N_d to the intermediate node N_u where $N_u^{LD} = N_d^{LD} - E_w$. An **availability interval** (α) is the time interval that object O_i wait at node N_u such that $\alpha(u) = [N_u^{EA}, N_u^{LD}] \neq \emptyset$, where $EA_i(u) \leq LD_i(u)$. A node N_u is defined as **reachable** when $\alpha(u) \neq \emptyset$ and **not reachable** if $\alpha(u) = \emptyset$ or $N_u^{EA} > N_u^{LD}$.

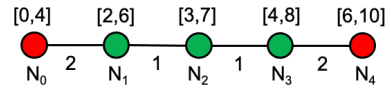


Figure 5: An illustration of Possible Rendezvous Nodes

Figure 5 shows nodes N_0 to N_4 with intervals $[0,4]$, $[2,6]$, $[3,7]$, $[4,8]$ and $[6,10]$ respectively. Nodes N_0 and N_4 are start and end nodes respectively and nodes $[N_1, N_2, N_3] \in N_u$. The earliest arrival is calculated by adding E_w to a given intermediate node N_u . For instance, $N_1^{EA} = N_0^{EA} + E_w(N_0, N_1) = 0 + 2 = 2$. Similarly, the values of N_2^{EA} , N_3^{EA} and N_4^{EA} are 3, 4 and 6 respectively. In contrast, the latest departure is calculated by subtracting E_w to a given intermediate node N_u . For instance, $N_4^{LD} = N_5^{LD} - d(N_5, N_4) = 10 - 2 = 8$. Similarly, the values of N_2^{LD} , N_3^{LD} and N_4^{LD} are 3, 4 and 6 respectively.

In the case of multiple paths P_s from a single source (i.e., N_s or N_e), shortest path algorithms (e.g., **Bi-directional Dijkstra's**) or other breadth first search approaches are considered. Hence, multiple arrival times and late departure times need to be considered for a given node N_i such that the earliest arrival time will be the **minimum** of all the arrival times derived via the shortest path from N_s to N_u (i.e., $\min([N_u^{EA_1}, N_u^{EA_2}, \dots, N_u^{EA_k}])$). In contrast, the latest departure time will be the **maximum** of all the departure times that result via the shortest paths from N_e to N_u (i.e., $\max([N_u^{LD_1}, N_u^{LD_2}, \dots, N_u^{LD_k}])$).

$$\alpha(N_u) = [\min([N_u^{EA_1}, \dots, N_u^{EA_k}]), \max([N_u^{LD_1}, \dots, N_u^{LD_k}])] \quad (14)$$

A **Possible Rendezvous Node** (N_R): is defined as a possible node N_u (or location) where two or more gaps belongs to different gaps could have physically met. For instance, the availability intervals of gaps G_i and G_j at N_u are defined as $\alpha(N_u, G_i)$ and $\alpha(N_u, G_j)$ respectively. The rendezvous is feasible only if :

$$\alpha(N_u, G_i) \cap \alpha(N_u, G_j) \geq TO \quad (15)$$

where $TO (\neq \emptyset)$ is defined as **Time Overlap threshold**.

If the above conditions are satisfied, the nodes are then the nodes are forwarded to human analysts for manual inspection.

4.1 Constructing Spatial Sub-networks

Section 3 describes how time slicing in an unconstrained (i.e., euclidean) space narrows down the search space through the construction of a lens at given time instant t to provide tighter bounds as compared to entire geo-ellipse region.

In spatial networks, we restrict such unconstrained movements which closely resembles an vehicle's mobility in a road network. However, we use the combination of geo-ellipses and lenses to geometrically restrict the object movement capabilities in a Manhattan search space, thereby providing an upper bound towards the mobility. In addition to tightening the spatial bounds, time slicing also capture the time-dependent properties of spatial networks which more accurately model an object's mobility in real-world scenarios.

Algorithm 1 first gathers trajectory gap pairs based on their temporal properties via a *Filter* and *Refine* approach to minimize the combinatorial computations. Then we temporally sample each trajectory gaps which captures a time-dependent edge which can later affects overall object's mobility.

4.1.1 Extract Trajectory Gap Pairs: For the effective gap collection, we use a *plane-sweep approach* to sort the trajectory gaps G_i and then filter out gaps that are not involved in a rendezvous. First, we sort all gaps $G_i \in [t_s, t_e]$ based on the start time t_s of the coordinates of G_i . Then, we filter gap pairs by checking the *necessary* condition i.e., whether their respective time ranges overlap. For instance, Gap G_i and G_j should satisfy their respective time ranges $[t_s^{G_i}, t_e^{G_i}]$ and $[t_s^{G_j}, t_e^{G_j}] \neq \emptyset$ (using Equation 2).

For the sufficient condition, we check if G_i and G_j are spatially intersecting such that $Ellipse_i \cap Ellipse_j \neq \emptyset$. If yes, then we save the resultant shape of $Ellipse_i \cap Ellipse_j$ and time range $[t_s^{G_i}, t_e^{G_i}] \cap [t_s^{G_j}, t_e^{G_j}] = [t_s^R, t_e^R]$ for creating spatial sub-networks.

4.1.2 Creating Spatial Sub-Networks: Here, we generate spatial sub-networks based on the qualifying nodes within the spatial (i.e., $Ellipse_1 \cap Ellipse_2$) and temporal $[t_s^R, t_e^R]$ constraints of the trajectory gap pairs $\langle G_1, G_2 \rangle$ as described in Section 4.1.1. To create a spatial network (SN), we perform a linear scan of (N) nodes and edges (E) $\in Ellipse_1 \cap Ellipse_2$ and to calculate edge weight E_w by considering historic location traces residing within the time range of $[t_s^R, t_e^R]$ and calculate the time cost by taking average speed μ (MS) and dividing it by total edge distance between N_i and N_j .

During time slicing, we capture the dynamic edge weights within $[t_s^R, t_e^R]$. First perform uniform sampling for a given temporal range into N samples where $[t_i^R, t_{i+1}^R] \in [t_s^R, t_e^R]$. We then compute edge weights E_w^i with given time range $[t_i^R, t_{i+1}^R]$ and filter nodes which are qualified within the $Lens_i$ where $N_i \subseteq N$. Hence for each time

frame we generate subnetworks SN_i with nodes N_u^i edge weights $E_w^i \forall i \in [t_i^R, t_{i+1}^R]$.

Algorithm 1 Spatial Sub-Networks with Rendezvous Gap Pairs

Input:

Historic Trajectory Data (HTD)
A set of Trajectory Gaps $[G_1, \dots, G_n]$
A Spatial Network N
A Sampling Rate K

Output:

Spatial Sub-Networks List

1: **procedure** :

2: Sub-Networks Map $\leftarrow \emptyset$

3: **for each**: $G_i \in$ Non-Observed List **do**:

4: **for each**: $G_j \in$ Observed list if Observed list $\neq \emptyset$ **do**

5: **if** $[t_s^{G_i}, t_e^{G_i}] \cap [t_s^{G_j}, t_e^{G_j}]$ and $G_i \cap G_j \neq \emptyset$ **then**:

6: $[SN_0, SN_1, \dots, SN_k] \leftarrow$ Subnetworks $(G_i \cap G_j, HTD, N, K)$

7: Sub-Networks Map $\leftarrow [G_i, G_j] \leftarrow [SN_0, SN_1, \dots, SN_k]$

8: **return** Sub-Networks Map

Algorithm 1 summarizes the process of gathering trajectory gap pairs and creation of spatial networks in steps as follows:

Step 1: For a given trajectory gap G_i in a Non-Observed list, we first check if G_i intersects with G_j in the Observed List $\neq \emptyset$. In case Observed List $\in \emptyset$, we add $G_i \in$ Observed List and move to G_{i+1} in the Non-Observed List. If G_j present in the Observed List, we check if the Ellipse bounds of $G_i \cap G_j$ and $[t_s^{G_i}, t_e^{G_i}] \cap [t_s^{G_j}, t_e^{G_j}] \neq \emptyset$. If not, then we derive intersected temporal range $[t_s^R, t_e^R] \in [t_s^{G_i}, t_e^{G_i}] \cap [t_s^{G_j}, t_e^{G_j}]$ and the resultant geo-ellipse intersection boundary of $(G_i \cap G_j)$ for unconstrained rendezvous study area which is later projected on a the given spatial network N to extract sub-network SN for gap pairs $\langle G_i, G_j \rangle$ where $SN \subseteq N$.

Step 2: For a given trajectory gap pair $\langle G_i, G_j \rangle$ and sampling rate K , we sample time interval $[t_s^R, t_e^R]$ in K samples such that each sub-network $SN_i, SN_{i+1}, \dots, SN_k$ has it's corresponding time-stamp $[t_i^R, t_{i+1}^R, \dots, t_{k-1}^R, t_k^R]$. Using historic trajectory data HTD, we calculate edge weights $E_w \forall SN$ using Equation ?? where each $SN_i \in \{E_w, t_k^R\}$ is then saved in Sub-Network Map which is later returned as the output.

4.2 Time Slicing Gap-Aware Rendezvous Detection Algorithm (TGARD)

The proposed TGARD algorithm captures an object's more realistic movements by considering parameters such as traffic congestion, which later affect the shortest path computation needed to calculate Earliest Arrival and Latest Departure time of the given sampled sub-network SN_k where each sub-network $SN_k \in [t_k^R]$ and $Lens_k$.

Intermediate nodes N_u is defined within $Lens_k^{G_i} \cap Lens_k^{G_j}$ towards which shortest path computation form start and end nodes is computed to calculate N_u^{EA} and N_u^{LD} . However, we need to perform shortest path computation for every N_u of every sampled sub-network SN_k and edge weights E_w^k . Figure 6 is a time aggregated graph representation [8] where each edge represents time series edge weights $[E_w^{t_1}, E_w^{t_2}]$, and $E_w^{t_1} \in P_1$ and $E_w^{t_2} \in P_2$, which gives the shortest path from N_0 to N_6 .

In Figure 6, P_1 takes the path N_0, N_1, N_4, N_5 , and N_6 at t_0 (since $2+1+1 \geq 3$). In contrast, path P_2 uses $N_0, N_1, N_2, N_3, N_4, N_5$ and N_6 since the path from N_1 and N_2 at t_1 is $5 \geq 2+1+1$ (i.e., N_1, N_2 ,

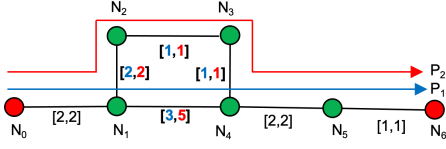


Figure 6: An illustration of Time Dependent Shortest Path

N_3 and N_4). In this case, node N_4 gets affected and the shortest path needs to be recomputed towards N_4 at time t_2 . To capture such changes in edge weights in $E_w^i \in t_i$ and $E_w^{i+1} \in t_{i+1}$, we use a difference metric $\delta(E_w^{i,i+1})$ and compare it with a threshold τ (i.e., whether $\delta(E_w^{i,i+1}) \geq \tau$). If it is, then we recompute the shortest path towards that node. In Algorithm 2, we denote $\delta(E_w^{i,i+1})$ as $\delta(E_w^k)$. For instance, in Figure 6, node N_4 gets affected at time $t = 2$ given $\tau = 2$ since $\delta(E_w^{i,i+1}) \geq \tau$. Hence we recompute the shortest path at P_2 from N_0 to N_6 via N_2 and N_3 . If not, the current path remains the same for future computations and thereby retains its optimal sub-structure property for shortest path, stated as follows:

THEOREM 4.1. *Given $G = (V, E)$ with edge weights E_w . Let $P = [N_1, N_2, N_3, \dots, N_k]$ be the shortest path from N_1 to N_k such that $1 \leq i \leq j \leq k$. If $P_{ij} = [N_i, N_{i+1}, \dots, N_j]$ is the sub-path of P from node N_i to N_j . Then, P_{ij} is the shortest path from P_i and P_j .*

Proof. The proof is straightforward. If we decompose P into $P_{1,j} \rightarrow P_{i,j} \rightarrow P_{j,k}$, where $E_w(P) = E_w(P_{1,j}) + E_w(P_{i,j}) + E_w(P_{j,k})$ and assume a new path P'_{ij} from N_i to N_j such that $E_w(P'_{ij}) \leq E_w(P_{ij})$. Then, $E_w(P) \leq E_w(P_{1,i}) + E_w(P'_{i,j}) + E_w(P_{j,k})$ which contradicts P as shortest path assumption from N_1 to N_k . \square

Algorithm 2 Time Slicing Gap-Aware Rendezvous Detection

Input:
Time Overlap Threshold TO
Rest same as Algorithm 1

Output:
Possible Rendezvous Nodes Hmap N_R

1: **procedure** :

2: Rendezvous Node Map $RNMap \leftarrow \emptyset$

3: Use Algorithm 1 to construct Subnetwork Map SN Map

4: **for each**: Sub Network $SN_k \in$ Trajectory Gap Pairs G_i, G_j **do**

5: Construct $Lens_k^{G_i}$ and $Lens_k^{G_j}$ for $t_k^R \in [t_s^R, t_e^R]$

6: **if** $Lens_k^{G_i} \cap Lens_k^{G_j} \neq \emptyset$ and $\delta(E_w^k) \leq \tau$ **then**:

7: $N_u \leftarrow Lens_k^{G_i} \cap Lens_k^{G_j}$

8: **if** N_u^k is reachable for Sub Network SN_k and $\notin RNMap$ **then**:

9: Compute N_u^{EA} and N_u^{LD} for both $\alpha(N_u^{G_i})$ and $\alpha(N_u^{G_j})$

10: **if** $\alpha(N_u^{G_i}) \cap \alpha(N_u^{G_j}) \neq \emptyset$ and $\geq TO$ **then**:

11: Rendezvous Node Map $RNMap[N_R] \leftarrow N_u \vee t_k^R$

return Rendezvous Node Map $RNMap$

The TGARD algorithm steps are as follows:

Step 1: First we compute a sub-network (SN) map for each gap pair $\langle G_i, G_j \rangle$ using Algorithm 1 and initialize a Rendezvous Node Map $RNMap \leftarrow \emptyset$. For each gap pair $\langle G_i, G_j \rangle$, we have k sub-networks SN_k which generate $Lens_k$ from both G_i and G_j at t_k^R . We then filter out N_u^k residing within the spatial boundary of $Lens_k^{G_i} \cap Lens_k^{G_j}$, where $Lens_k^{G_i} \cap Lens_k^{G_j} \neq \emptyset$. In addition, we also check if edge weights $\delta(E_w^k)$ for sub-network SN_k have changed considerably by comparing them with threshold τ . If yes, then we

consider all the affected nodes within $Lens_k^{G_i} \cap Lens_k^{G_j}$ for computing *early arrival* and *late departure* times to preserve completeness. If not, we re-use the previous shortest path calculations for *early arrival* and *late departure* at t_{k-1}^R adhering to the optimal substructure property for a shortest path stated in Theorem 4.1.

Step 2: After gathering all $N_u \in Lens_k^{G_i} \cap Lens_k^{G_j}$, we check if N_u is reachable (i.e., $\alpha(N_u) \neq \emptyset$) by checking the availability interval $[N_u^{EA}, N_u^{LD}] \not\subseteq [t_s, t_e]$ for each gap G_i and G_j . If valid, we then check whether both the availability intervals of G_i and G_j and their intersection is $\neq \emptyset$ and $\geq TO$. If yes, then N_u^k qualifies as N_R and is saved in a rendezvous node (RN) Map which is later returned as output.

4.3 A Dual Convergence Approach (DC-TGARD)

Since time slicing operation is computationally expensive, the Dual Convergence method leverage symmetric property of the ellipse to efficiently reduce the iterations of time slicing used by TGARD while preserving correctness and completeness. We first define an early termination condition based on areal coverage of $Lens_k$, where $k \in 0 \leq k \leq n$ for a given time frame t , where $t \in 0 \leq k \leq n$. We then perform *bi-directional pruning* using ellipse symmetric property and compute *EA* and *LD* from both tail-end of the ellipse in parallel to improve computational efficiency.

Ellipse Symmetry Property: Given ellipse with major and minor axis and center $(0,0)$, then its foci $(\pm c, 0)$ are equidistant from its origin at c . Hence, the areal coverage drawn from the lenses centered at $(\pm c, 0)$ will be the same, permitting an equal number of nodes within the spatial bounds of the lenses. For instance, Figure 7 (b) shows an equal number of nodes residing within the spatial bounds of $Lens_k$ and $Lens_{n-k}$ and using Lemma 3.3, time slicing does not leave out any other interpolated nodes (green) bounded within ellipse preserving the completeness of DC-TGARD.

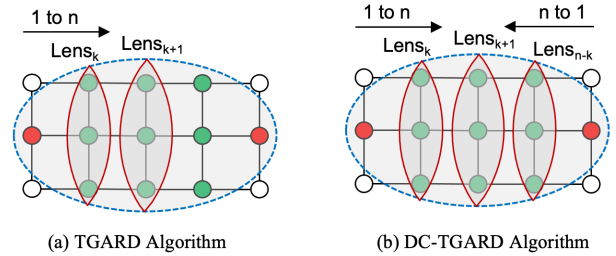


Figure 7: An illustration of TGARD vs Dual Convergence Method

Early Stopping Criteria: The early stopping criteria holds when the property of monotonicity (i.e., non-increasing) is violated while estimating the areal coverage of lenses throughout every time slicing operation from t_s to t_e . For instance, Figure 7 (a), shows the increasing areal-coverage i.e., $A(Lens_k) \leq A(Lens_{k+1})$ (given $A(Lens_k)$ as the areal coverage of lens k at t_k and t_{k+1} respectively (where, $t_{k+1} \geq t_k$). This is due to the increasing (or non-decreasing) length of the minor axis which preserves the monotonicity until the $Lens_{k+1}$ of the ellipse. After $Lens_{k+1}$, the areal coverage start decreasing and thereby violating the monotonic property i.e.,

($A(Lens_k) \leq A(Lens_{k+1}) \geq A(Lens_{i+2})$) and, resulting in early stopping of the time slicing operation.

Dual Convergence Approach: We need to consider each time-slice operation to preserve completeness of the algorithm. The dual convergence approach introduces **bi-directional pruning** in conjunction to efficiently converge towards *early stopping criteria*. Hence, a time-slicing operation is performed from both tail ends of the ellipse foci in parallel such that both lenses generated at t and $t_e - t$ follows the property of **ellipse symmetry**. While performing bi-directional pruning, we check the *early stopping criteria* if $A(Lens_i) \geq A(Lens_{i+1})$ such that the monotonic property is violated. Figure 7 shows an example of dual convergence where baseline TGARD in Figure 7 (a) performs a linear time slicing operation from $Lens_k$, $Lens_{k+1}$ to $Lens_n$ covering all the interpolated nodes. Figure 7 (b) shows bi-directional pruning at $Lens_k$ and $Lens_{n-k}$ where $k \in [1, n]$. The areal coverage of $Lens_k$ i.e., $A(Lens_k)$ and $A(Lens_{n-k})$ using the property of ellipse symmetry computed in parallel and further checking if $A(Lens_k) \geq A(Lens_{k+1})$ which gives an early stopping condition. For instance, in Figure 7 DC-TGARD terminates when $A(Lens_{k+1}) \geq A(Lens_{n-k})$ at $t=2$ as compared to TGARD in Figure 7 (a) which terminates at $t=3$. Hence, the areal coverage pruning is more efficient in DC-TGARD as compared to TGARD. Hence the pruning is similar to a *bitonic array* where the peak areal coverage using *MaxOverlap* variable.

Algorithm 3 Dual Convergence Time Slicing Gap-Aware Rendezvous Detection (DC-TGARD)

Input:
Same as Algorithm 2

Output:
Possible Rendezvous Nodes List N_R

```

1: procedure :
2:   Use Algorithm 1 to construct Subnetwork Map SN Map
3:   Rendezvous Node Map RNMap  $\leftarrow \emptyset$  and Max Overlap  $\leftarrow \emptyset$ 
4:   Construct Sub Network  $SN_k$  and  $SN_{n-k}$  for  $t_k^R$  and  $t_{n-k}^R$  respectively
5:   for each: Sub Network  $SN_k$  and  $SN_{n-k} \in$  Trajectory Gap Pairs  $\langle G_i, G_j \rangle$  do
6:     Construct  $Lens_k^{G_i}, Lens_k^{G_j} \in t_k^R$  and  $Lens_{n-k}^{G_i}, Lens_{n-k}^{G_j} \in t_{n-k}^R$ 
7:     while Max Overlap  $\not\geq$  Area( $Lens_k^{G_i} \cap Lens_k^{G_j}$ ) do
8:       if  $Lens_k^{G_i} \cap Lens_k^{G_j} \neq \emptyset$  and  $\delta(E_w^k, E_w^{n-k}) \leq \tau$  then
9:          $N_u^k \leftarrow Lens_k^{G_i} \cap Lens_k^{G_j}$  and  $N_u^{n-k} \leftarrow Lens_{n-k}^{G_i} \cap Lens_{n-k}^{G_j}$ 
10:        if  $N_u^k \in SN_k$  and  $N_u^{n-k} \in SN_{n-k}$  reachable and  $\notin$  RNMap then:
11:          Compute  $N_u^{EA}, N_u^{LD} \vee t_k^R$  and  $t_{n-k}^R \in \alpha(N_u^{G_i})$  and  $\alpha(N_u^{G_j})$ 
12:          if  $\alpha(N_u^{G_i})$  and  $\alpha(N_u^{G_j}) \neq \emptyset$  and  $\geq TO \vee t_k^R$  and  $t_{n-k}^R$  then:
13:            Rendezvous Node Map RNMap[ $N_R$ ]  $\leftarrow N_u^k$  and  $N_u^{n-k}$ 
14:   return Rendezvous Node Map RNMap

```

The DC-TGARD algorithm steps are as follows:

Step 1: After generating Sub-Network Map (SN Map) via Algorithm 1, we first initialize Rendezvous Node Map RNMap and Max Overlap variable as \emptyset . We then generate sub-networks SN_k and SN_{n-k} for each t_k^R and t_{n-k}^R and generate $Lens_k$ and $Lens_{n-k} \subseteq SN_k$ and SN_{n-k} respectively. We then check if $Lens_k^{G_i}, Lens_k^{G_j} \cap Lens_{n-k}^{G_i}, Lens_{n-k}^{G_j} \leftarrow \emptyset$ and simultaneously check $\delta(E_w^k, E_w^{n-k})$ with threshold τ . Rest of the steps are similar to TGARD instead we simultaneously calculate every variables for early arrival, late departures and availability intervals along with their respective conditions.

Step 2: We update the Max Overlap variable with Area of $Lens_k^{G_i} \cap Lens_k^{G_j}$ or $(Lens_{n-k}^{G_i} \cap Lens_{n-k}^{G_j})$. Finally, we check the early termination condition (i.e., current $Lens_k^{G_i} \cap Lens_k^{G_j}$ and $Lens_{n-k}^{G_i} \cap Lens_{n-k}^{G_j} \geq$ Max Overlap. If yes, then the loop has reaches to the *peak element* and algorithm terminates.

5 THEORETICAL EVALUATION

5.1 Correctness and Completeness

In this section, we provide a theoretical analysis of the correctness and completeness of the proposed algorithms.

LEMMA 5.1. *TGARD and DC-TGARD algorithms are correct.*

Proof. Given a finite set of $|K|$ trajectories with maximum N number of finite points resulting in a maximum bound of $|K| \times |N|$ finite trajectory points. Hence, finite number of trajectory gaps G_i generated while performing pre-processing for finite trajectory gap-pair generation resulting a finite number of operations will be performed by *TGARD and DC-TGARD* algorithms to terminate at a finite time. The correctness of the algorithm also depends upon the extent of the overlap of the two availability intervals $\alpha(1) \in G_1$ and $\alpha(2) \in G_2$. For instance, a low overlap threshold results in multiple false positive rendezvous whereas a high overlap threshold results in more false negatives. Hence, both *TGARD and DC-TGARD* algorithms are correct for a given overlap threshold. \square

LEMMA 5.2. *TGARD and DC-TGARD algorithms are complete.*

Proof. The proposed *TGARD and DC-TGARD* algorithms consider all the nodes within the spatial bounds of the lenses and their respective geo-ellipses. Theorem 3.3 proved that a time slice lens is a subset of geo-ellipse and does not exceed its limit. This ensures that each node within gap is participating during time slicing operation. Hence, both *TGARD and DC-TGARD* algorithms are complete. \square

5.2 Asymptotic Analysis

The time complexity of the comparison operations for each algorithm are as follows:

Exacting Candidate Gap Pairs: For generating candidate pairs, $\binom{|K|}{2}$ trajectories must be selected where each such pair will have $|N-1| \times |N-1|$ comparisons. Hence, the total number of comparisons will be $\binom{|K|}{2} \times |N-1| \times |N-1|$, which results in an asymptotic worst case of $O(|K|^2 \times |N|^2)$.

Creating Sub-Networks (SNs): For a given subgraph SN with $|E| \subseteq N \times N$ edges, the edge weights needs to be calculated $|T|$ times where E_w is calculated at constant time. Hence the overall time complexity for calculating E_w is $O(|E| \times |T|)$.

TGARD Algorithm: Given a sub-network SN for N nodes, we perform a linear scan for each time slice $|T|$ to gather intermediate node N_u where $N_u \leq N$ resulting in $O(|K| \times |T|)$ operations. For computing Early Arrival and Late Departure for N_i , we run a *bi-directional Dijkstra's* algorithm with $O(|N_i| + |E|)$. Hence, the algorithm perform $O(|K| \times |T|) + O(|N_u| \times |E|)$ operations.

DC-TGARD Algorithm: The worst case of DC-TGARD will be similar to *TGARD* except we perform bi-directional searches while computing the time slice operations and the early termination condition guarantees the algorithm stops in $T/2$ steps. This in turn

reduces shortest path computations, which enhances computational efficiency in high density regions.

6 EXPERIMENTAL EVALUATION

The goal of the experiments was to validate the benefit of the proposed time slicing approach for reducing the search space of rendezvous detection. We evaluated the solution quality by comparing the proposed DC-TGARD against space-time prism methods [23]. We also compared the execution time of TGARD and DC-TGARD under different parameters. Details shown in Fig 8.

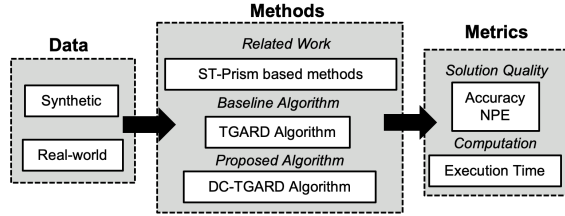


Figure 8: Experiment Design

Real World Data: We used Geolife [29] dataset based on Beijing Road Networks where each location has latitude, longitude, and height with a variety of travel modes (e.g., walking, driving, etc.). In this paper, we limited our evaluation to driving patterns due to their accordance with road network topology (e.g., road segment and intersection). In addition, we further simulated certain trajectories by adding more objects and case scenarios of rendezvous patterns to test the effectiveness and scalability of the proposed methods.

Synthetic Data Generation: For *solution quality* experiment, we lacked ground truth data (i.e., information on whether a node was involved in a rendezvous or not). Therefore, we evaluated the proposed algorithms on synthetic data derived from the Geolife dataset. First, we gather trajectories on a fixed study area of the Beijing road network with mobility data. We then pre-processed the trajectory points with gap durations greater than 30 mins and randomly classified each gap based on whether N_r was reachable or was not using the proposed methods.

Computing Resources: We performed our experiments on a system with a 2.6 GHz 6-Core Intel Core i7 processor and 16 GB 2667 MHz DDR4 RAM.

6.1 Solution Quality

To assess solution quality, we considered bounding efficiency and accuracy. We developed an efficiency metric called node pruning efficiency (NPE), to measure the tightness of the proposed filter in the trajectory gap pairs. We defined NPE as the ratio of the nodes of a total study area to the nodes within a bounded region (Eq. 16):

$$NPE = \frac{\text{Nodes in Total Study Area}}{\text{Nodes in the Bounded Region}} \quad (16)$$

Nodes Pruning Efficiency (NPE): We fixed the study area and varied the Nodes (N), Effective Missing Period (EMP), Speed (MS) and Number of Objects (O) within each trajectory gap G_i . Figure 9 shows the results for the space-time prism approach and the proposed time slicing approach. As can be seen in Figure 9 (a), DC-TGARD has better node pruning efficiency (NPE) as we increase

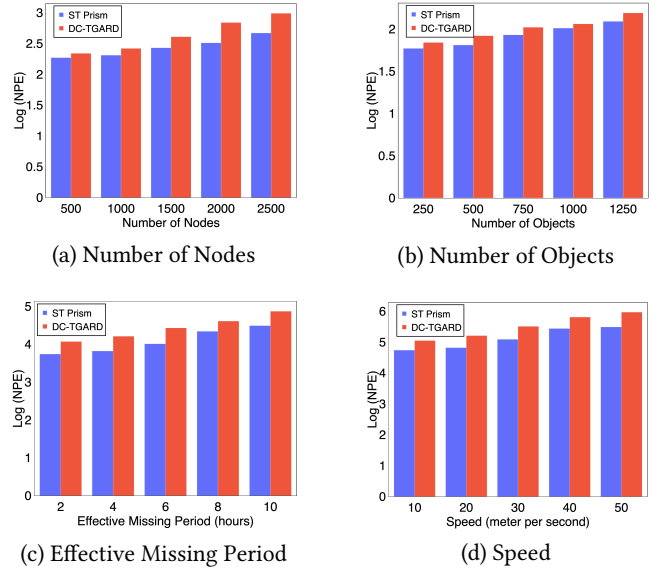


Figure 9: DC-TGARD performs better than a space-time prism method under different parameters

the number of nodes (since node density increases). A similar trend is seen in Figure 9 (b) except the effectiveness of time slicing is not as significant as we increase the number of objects of a fixed study area. Figure 9 (c) and 9 (d) again show the time slicing effectiveness is superior as compared to baseline approach as we increase the duration of the effective missing period (EMP) of gap.

Accuracy: We used synthetic data with manually labelled ground truth data about whether or not the objects were involved in rendezvous for a fixed number of objects (i.e., 2000) within a fixed size network of 5000 nodes. We then varied different parameters including Time Overlap Threshold (TO).

(1) **Number of Objects:** We set the EMP to 4 hours, MS to 30 m/s , Time Overlap Threshold (T) to 30 mins and we varied the number of objects from 500 to 1250. Figure 10 (a) shows DC-TGARD gives a more accurate representation of the minimum travel time from the start node and end node of the trajectory gap compared to space-time prism based methods. This results in more accurate estimates of N_r and reduces the number of false negatives, which proved to be quite common in the space-time prism based approaches [23].

(2) **Effective Missing Period (EMP):** Next, we set the number of objects at 500, the number of nodes of 5×10^4 , MS at 30 m/s , TO threshold to 30 mins, and varied the EMP threshold from 2 to 10 hours. As shown in Figure 10 (b), we find that DC-TGARD outperforms space time prisms. Higher EMP estimates increase the size of the geo-ellipses resulting in higher false positives.

(3) **Speed:** We kept the number of objects and EMP constant at 1000 and 4 hours respectively, the TO threshold at 30 mins and increased the maximum speed MS from 10 to 50 in *meter/second* units. Figure 10 (c) shows DC-TGARD is more accurate as compared to ST-Prisms. The reason is that high speed outputs a greater number of potential rendezvous. This increases false positives on

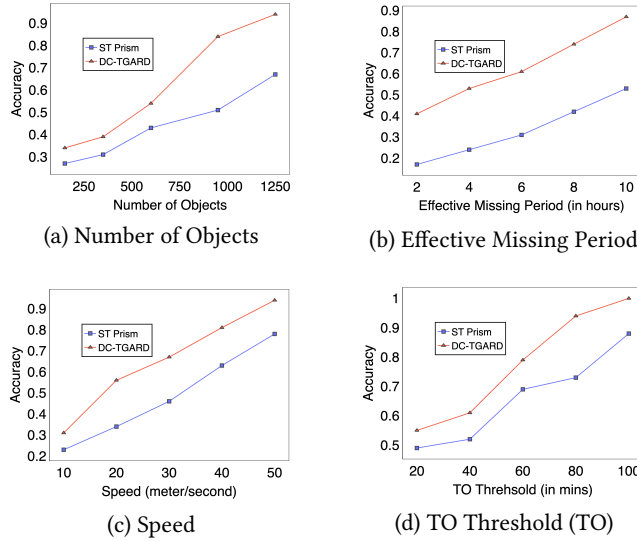


Figure 10: DC-TGARD is more accurate ST Prism under varying parameters
both algorithms but DC-TGARD filters out *non-reachable* nodes, thereby increasing accuracy.

(4) **Time Overlap Threshold (TO):** We set EMP at 4 hours, MS at 30 *m/s* and varied the TO threshold from 20 min to 100 mins. Again, DC-TGARD outperforms space-time prism as we increase TO threshold (Figure 10 (d)). We also see that greater TO threshold results in less N_r , resulting in more false negatives which are more accurately captured by the proposed DC-TGARD algorithm.

6.2 Computational Efficiency

We then compared the proposed DC-TGARD against the baseline TGARD algorithm on computation efficiency using Number of Nodes, Number of Objects, Effective Missing Period, Speed MS and Time Overlap Threshold (TO).

(1) **Number of Objects:** We set the EMP to 4 hours, MS to 30 *m/s*, Time Overlap Threshold (T) to 30 mins and we varied the number of objects from 500 to 2500. Figure 11 (a) shows that DC-TGARD always runs faster than TGARD algorithm it's dual-convergence time-slicing operation leverages early stopping criteria.

(2) **Effective Missing Period (EMP):** We set the number of objects at 500, the number of nodes of 5×10^4 , MS at 30 *m/s*, TO threshold to 30 mins, and varied the EMP from 30 to 90 minutes. As shown in Figure 11 (b), we find that DC-TGARD outperforms TGARD with increasing EMP. The bi-directional pruning of the dual convergence approach reduces the time slicing operations.

(3) **Speed:** We kept the number of gaps and EMP constant at 1000 and 4 hours respectively, TO threshold 30 mins and increased the maximum speed MS from 10 to 50 in *m/s* units. Figure 11 (c) shows DC-TGARD is faster than TGARD. Hence, the dual convergence of DC-TGARD helps but not that significantly if we increase the MS. The reason is similar to EMP results since higher maximum speed produces larger ellipses except non-reachable nodes the non-reachable nodes decreases for both the algorithms which results in more shortest path computations for both algorithms.

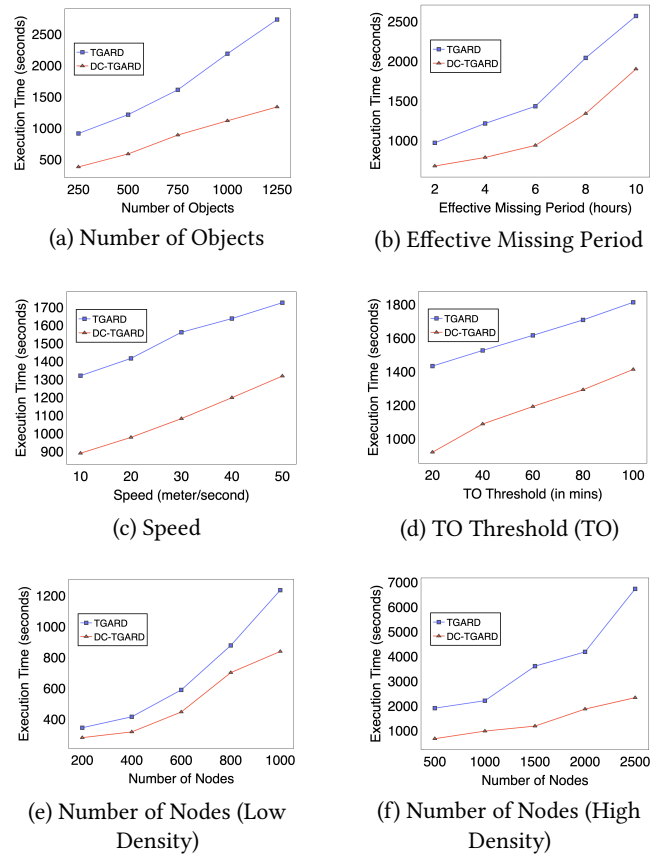


Figure 11: DC-TGARD is more efficient than TGARD Methods under different parameters

However, DC-TGARD outperform due to it's dual convergence property, the execution times for both algorithms are linear as the speed increases.

(4) **Time Overlap Threshold (TO):** We again kept the number of objects at 1000, the EMP at 4 hours, MS at 30 *m/s* but this time we increased the TO threshold from 20 min to 100 mins. Again, Figure 11 (d) shows DC-TGARD outperforms TGARD as we increase TO threshold i.e., the dual convergence nature of DC-TGARD efficiently filter out more N_r and fewer shortest path computations are performed.

(5) **Number of Nodes:** We did a high density test by setting the number of objects to 1000 and varied the number of nodes from 500 to 2500. For low density test, we set the number of objects to 100 and varied number of nodes from 200 to 1000. For both experiments, EMP was set to 4 hours, MS to 30 *m/s* and Time Overlap Threshold (TO) to 40 mins for a fixed study area. Figure 5 (e) and (f) shows that DC-TGARD always outperforms the TGARD algorithm. It's time slicing operations are effective for both high and low density road networks.

7 OTHER RELATED WORK

The literature of trajectory mining includes a broad overview of movement patterns [6] and a taxonomy of spatial mining methods used in various application domains [28]. In trajectory data management, specific frameworks have analyzed trajectory gaps via indexing methods (e.g., hierarchical trees [2, 10], grids [18] but they are not designed to detect movement patterns. Other works have modelled regions of uncertainty [20, 22] via snapshot models etc. More realistic solutions are based on geometric models such as cylindrical [21] and space-time prism models [9, 13, 17] that construct an areal interpolation of the gaps using coordinates and a maximum speed of the objects. More recently, a kinetic prism [14] approach showed improved estimation by considering other physical parameters (e.g., acceleration). However, no studies have addressed rendezvous behavior patterns within trajectory gaps.

In spatial network research, many methods consider [7, 16, 24] uncertainty in trajectory gaps by a map matching the potential routes taken by a moving object in a road network. Many studies are based on deterministic [26, 27] and probabilistic [11, 12] methods that consider historic trajectories to find potential routes in a road network topology. However, none of these works consider rendezvous behavioral patterns in spatial networks. Recent work [23], studies rendezvous detection in the *static-spatial network* via space-time prisms based on objects and duration using type-2 uncertainty (geo-ellipse) resulting rather loose bounds. In this work, we are identifying rendezvous nodes via a time-slicing method [19] which tighten the bounds of rendezvous areas. We further consider dynamic edge weights [3, 4, 25] for better solution quality.

8 CONCLUSION AND FUTURE WORK

We study the problem of identifying a set of possible rendezvous locations within a trajectory gap in a given spatial network. We theoretically study a time slicing model which provides tighter bounds as compared to traditional space-time prism models. We also proposed a TGARD algorithm for effectively finding rendezvous nodes while filtering non-reachable nodes in the spatial networks to improve solution quality. In addition, we refined our baseline approach with a Dual Convergence TGARD (DC-TGARD) algorithm using bi-directional pruning to further improve computational efficiency. Experimental results on both synthetic and real-world datasets shows that DC-TGARD is faster than TGARD and has better solution quality than other related work based methods.

Future Work: In the future, we plan to investigate the adjustments of the proposed algorithm needed to handle possibly negative travel costs. We also plan to examine whether parallelism can be used to further improve query processing. Finally, we intend to develop a more accurate prism model to calibrate realistic physics-based parameters (e.g., acceleration).

ACKNOWLEDGMENTS

This research is funded by an academic grant from the National Geospatial-Intelligence Agency (Award No. HM0476-20-1-0009, Project Title: Identifying Aberration Patterns in Multi-attribute Trajectory Data with Gaps). Approved for public release, 22-536. We also want to thank Kim Koffolt and the spatial computing research group for their helpful comments and refinements.

REFERENCES

- [1] BBC. 2017. North Korea: South seizes ship amid row over illegal oil transfer. <https://www.bbc.com/news/world-asia-42510783>.
- [2] Su Chen, Beng Chin Ooi, Kian-Lee Tan, and Mario A Nascimento. 2008. ST2B-tree: a self-tunable spatio-temporal B+-tree index for moving objects. In *Proceedings of the 2008 ACM SIGMOD international conference on Management of data*. 29–42.
- [3] Ugur Demiryurek, Farnoush Banaei-Kashani, Cyrus Shahabi, and Anand Ranganathan. 2011. Online computation of fastest path in time-dependent spatial networks. In *International Symposium on Spatial and Temporal Databases*. Springer, 92–111.
- [4] Bolin Ding, Jeffrey Xu Yu, and Lu Qin. 2008. Finding time-dependent shortest paths over large graphs. In *Proceedings of the 11th international conference on Extending database technology: Advances in database technology*. 205–216.
- [5] Hui Ding, Goce Trajcevski, and Peter Scheuermann. 2008. Efficient similarity join of large sets of moving object trajectories. (2008), 79–87.
- [6] S Dodge, R Weibel, and A. Lautenschütz. 2008. Towards a taxonomy of movement patterns. *Information visualization* 7, 3-4 (2008), 240–252.
- [7] Joshua S Greenfeld. 2002. Matching GPS observations to locations on a digital map. In *Transportation Research Board 81st Annual Meeting*, Vol. 22.
- [8] Venkata Gunturi, Ernesto Nunes, KwangSoo Yang, and Shashi Shekhar. 2011. A critical-time-point approach to all-start-time lagrangian shortest paths: A summary of results. In *International Symposium on Spatial and Temporal Databases*. Springer, 74–91.
- [9] Hyun-Mi Kim and Mei-Po Kwan. 2003. Space-time accessibility measures: A geocomputational algorithm with a focus on the feasible opportunity set and possible activity duration. *Journal of geographical Systems* 5, 1 (2003), 71–91.
- [10] George Kollios, Dimitrios Gunopulos, and Vassilis J Tsotras. 1999. On indexing mobile objects. In *Proceedings of the eighteenth ACM SIGMOD-SIGACT-SIGART Symposium on Principles of Database Systems*. 261–272.
- [11] John Krumm, Robert Gruen, and Daniel Delling. 2013. From destination prediction to route prediction. *Journal of Location Based Services* 7, 2 (2013), 98–120.
- [12] John Krumm and Eric Horvitz. 2006. Predestination: Inferring destinations from partial trajectories. In *UbiComp*. Springer, 243–260.
- [13] Bart Kuijpers, Rafael Grimson, and Walied Othman. 2011. An analytic solution to the alibi query in the space-time prisms model for moving object data. *International Journal of Geographical Information Science* 25, 2 (2011), 293–322.
- [14] B. Kuijpers, H. J. Miller, and W. Othman. 2017. Kinetic prisms: incorporating acceleration limits into space-time prisms. *IJGIS* 31, 11 (2017), 2164–2194.
- [15] Bart Kuijpers and Walied Othman. 2009. Modeling uncertainty of moving objects on road networks via space-time prisms. *IJGIS* 23, 9 (2009), 1095–1117.
- [16] Yin Lou, Chengyang Zhang, Yu Zheng, Xing Xie, Wei Wang, and Yan Huang. 2009. Map-matching for low-sampling-rate GPS trajectories. In *Proceedings of the 17th ACM SIGSPATIAL international conference on advances in geographic information systems*. 352–361.
- [17] H. J. Miller. 1991. Modelling accessibility using space-time prism concepts within geographical information systems. *International Journal of Geographical Information System* 5, 3 (1991), 287–301.
- [18] Jignesh M Patel, Yun Chen, and V Prasad Chakka. 2004. STRIPES: an efficient index for predicted trajectories. In *Proceedings of the 2004 ACM SIGMOD international conference on Management of data*. 635–646.
- [19] Arun Sharma and Shashi Shekhar. 2022. Analyzing Trajectory Gaps to Find Possible Rendezvous Region. *ACM Transactions on Intelligent Systems and Technology (TIST)* 13, 3 (2022), 1–23.
- [20] Goce Trajcevski. 2003. Probabilistic range queries in moving objects databases with uncertainty. In *Proceedings of the 3rd ACM international workshop on Data engineering for wireless and mobile access*. 39–45.
- [21] Goce Trajcevski et al. 2010. Uncertain range queries for necklaces. In *2010 Eleventh International Conference on Mobile Data Management*. IEEE, 199–208.
- [22] Goce Trajcevski, Ouri Wolfson, Klaus Hinrichs, and Sam Chamberlain. 2004. Managing uncertainty in moving objects databases. *ACM Transactions on Database Systems (TODS)* 29, 3 (2004), 463–507.
- [23] Reaz Uddin, Michael N Rice, China V Ravishankar, and Vassilis J Tsotras. 2017. Assembly queries: Planning and discovering assemblies of moving objects using partial information. In *Proceedings of the 25th ACM SIGSPATIAL International Conference on Advances in Geographic Information Systems*. 1–10.
- [24] Jing Yuan, Yu Zheng, Chengyang Zhang, Xing Xie, and Guang-Zhong Sun. 2010. An interactive-voting based map matching algorithm. In *2010 Eleventh international conference on mobile data management*. IEEE, 43–52.
- [25] Liang Zhao, Tatsuya Ohshima, and Hiroshi Nagamochi. 2008. A* algorithm for the time-dependent shortest path problem. In *WAAC08: The 11th Japan-Korea Joint Workshop on Algorithms and Computation*.
- [26] Kai Zheng, Goce Trajcevski, Xiaofang Zhou, and Peter Scheuermann. 2011. Probabilistic range queries for uncertain trajectories on road networks. In *Proceedings of the 14th International Conference on Extending Database Technology*. 283–294.
- [27] Kai Zheng, Yu Zheng, Xing Xie, and Xiaofang Zhou. 2012. Reducing uncertainty of low-sampling-rate trajectories. In *2012 IEEE 28th ICDE*. IEEE, 1144–1155.

- [28] Y. Zheng. 2015. Trajectory data mining: an overview. *ACM Transactions on Intelligent Systems and Technology (TIST)* 6, 3 (2015), 1–41.
- [29] Yu Zheng, Xing Xie, Wei-Ying Ma, et al. 2010. GeoLife: A collaborative social networking service among user, location and trajectory. *IEEE Data Eng. Bull.* 33, 2 (2010), 32–39.